Available online at www.sciencedirect.com
SCIENCE DIRECT
Journal of Crystal Growth 290 (2006) 307–312
JOURNAL OF CRYSTAL GROWTH
www.elsevier.com/locate/jcrysgro

Novel yttria-stabilised zirconia–alumina tetragonal phase obtained by co-precipitation

J. Santoyo-Salazar[a,*], G. Gonzalez[a], J.A. Ascencio[b], J. Tartaj-Salvador[c], J.A. Chávez-Carvayar[a]

[a]*Instituto de Investigaciones en Materiales, UNAM, Circuito Exterior. C.U.A. Postal 70–360. Delegación Coyoacán. C.P. 04510. México D.F.*
[b]*Instituto Mexicano del Petróleo. Eje Central Lázaro Cárdenas 152. San Bartolo Atepehuacan. C.P. 07730. México D.F.*
[c]*Instituto de Cerámica y Vidrio, CSIC. Madrid, España*

Received 23 June 2005; received in revised form 21 January 2006; accepted 23 January 2006

Communicated by M.S. Goorsky

Abstract

Yttria-stabilised zirconia–alumina (YSZ–A) compounds, $\frac{90}{10}$, $\frac{80}{20}$, $\frac{70}{30}$ and $\frac{60}{40}$ wt%, were obtained by the co-precipitation route. Among them, a novel tetragonal phase, 90 wt% of 3 mol% YSZ and 10 wt% of Al_2O_3, was obtained. Phase identification was carried out by X-ray diffraction (XRD). For structural studies, XRD data were analysed by Rietveld refinements. This novel phase, with lattice parameters $a = 5.09964$ Å and $c = 5.17488$ Å, may be associated with a distorted polyhedron of a cubic ZrO_2 structure obtained by partial substitution of Y^{3+} and Al^{3+} cations at Zr^{4+} positions. Particle size, which was determined by transmission electron microscopy, ranges from 50 to 100 nm. Conductivity measurements, by impedance spectroscopy, showed a good ionic conductor material with similar properties of those of pure zirconia. Quantum mechanics molecular simulation determined the electron properties of the corresponding crystal. This allowed establishing the density of states, which implies important differences to the reported tetragonal phases.

Keywords: A1. Co-precipitation; A1. Density of states; A1. Impedance spectroscopy; A1. Rietveld refinement; A1. X-ray diffraction.

1. Introduction

Zirconia-based ceramics have received special attention due to their potential applications in a number of devices, like ion conductors in solid oxide fuel cells, oxygen sensors and catalytic appliances [1–5]. These compounds can be prepared by the addition of metallic oxides, MO and M_2O_3, in appropriate proportions to generate vacancies in the oxygen sub-lattice [1–6] by the replacement of zirconia cations by less charge cations [6–8]. Specially, yttria (Y_2O_3) and alumina (Al_2O_3) are oxides with high stability and mechanical strength at high temperature whose cations exhibit lower valence compared to that of Zr^{4+}. Nevertheless, ionic size radii of Al^{3+} (0.53 Å) is too small to substitute Zr^{4+} (0.84 Å) to be coordinated with eight oxide ions in tetragonal and cubic ZrO_2 [9].

To obtain a stable ZrO_2/Al_2O_3 compound it is important to get a homogenous dispersion of Al_2O_3, however the high concentration or a heterogeneous dispersion of alumina may affect the physical properties of the product. The incorporation of aluminium oxide in the ZrO_2 lattice may be controlled by the use of a soft route like sol–gel or co-precipitation. With these techniques, homogeneous crystalline materials with a small particle size and a high density can be prepared and then it is possible to improve the physical properties of synthesised materials [10–14].

In this work a soft route of synthesis, by fine dispersion powder in reactive solutions, was used to obtain a family of YSZ–Al_2O_3 ($\frac{90}{10}$, $\frac{80}{20}$, $\frac{70}{30}$ and $\frac{60}{40}$ wt%) compounds. A novel tetragonal phase YSZ–Al_2O_3, $\frac{90}{10}$ wt% (YSZ–A) was obtained. With the co-precipitation method, it was possible to synthesise this novel phase with a homogeneous distribution of aluminium atoms in the lattice. Samples were

*Corresponding author. Tel.: +52 55 5622 46 38; fax: +52 55 5616 13 71.
E-mail address: sjimmy@universo.com (J. Santoyo-Salazar).

0022-0248/$ - see front matter © 2006 Elsevier B.V. All rights reserved.
doi:10.1016/j.jcrysgro.2006.01.032

characterised by X-ray diffraction (XRD), Rietveld refinement, transmission electron microscopy, impedance spectroscopy and quantum mechanics based molecular simulation.

2. Experimental procedure

2.1. Preparation of the samples

In all 3 mol% yttria-stabilised ziconia/alumina, (3YSZ)/Al_2O_3, products were prepared with $\frac{90}{10}$, $\frac{80}{20}$, $\frac{70}{30}$ and $\frac{60}{40}$ wt% concentrations, respectively, by the co-precipitation route. The starting Al_2O_3 precursor was obtained by mixing $Al(NO_3)_3 \cdot 9H_2O$ aluminium nitride in ionised water. To obtain tetragonal zirconia, crystalline particles of 3 mol% yttria partially stabilised zirconia (TZ-3Y-E, Tosoh Zirconia Powder, Tosoh Corporation) were suspended in ionised water and added into the transparent dissolution of $Al(NO_3)_3 \cdot 9H_2O$, in proportions of 10, 20, 30 and 40 wt% Al_2O_3. To precipitate the Al^{3+}, NH_4OH was diluted at 50% with the precursor solution, pH = 9, with a constant stirring during the process. After the reaction, the precipitated and particles of 3 mol% YSZ–Al_2O_3 were washed with ionised water and pure ethanol to reduce the water amount and capillarity between the particles. Powders were dried at 90 °C, grounded and then fired at 300 °C for 20 h. Pellets of 0.4 g, 13 mm diameter and 0.5 mm thick, were prepared by cold-pressed powders under 150 MPa. Samples were sintered at 1100 °C in air for 2, 6 and 15 h.

2.2. Physical characterisation

Phase identification of 3%YSZ/Al_2O_3 ($\frac{90}{10}$, $\frac{80}{20}$, $\frac{70}{30}$ and $\frac{60}{40}$ mol%) compounds were carried out by XRD. Data were collected with a Bruker-AXS D8 Advance diffractometer, using CuKα radiation, $\lambda = 1.54056$ Å, at 35 kV and 30 mA. The scanned range was 10–80° 2θ, with a step of 0.02° 2θ and 1.2 s/step. For accurate determination of lattice parameters and for structural studies of the new phase, the scanned range was 10–120° 2θ, with a step of 0.02° 2θ and 10 s/step.

For structural refinements, from X-ray powder diffraction data, the FULPROF-Suite program was used as Rietveld software [15]. The background was approximated by a linear interpolation of 70 data points. The profile function, which was used to describe the peak shape, was a Thompson–Cox–Hastings pseudo-Voigt function. Instrumental profiles, based on LaB_6 standard, were incorporated to the refinement.

Transmission electron microscopy (TEM) (JEM1200EX, JEOL), was used to analyse the particle size and also to study the electron diffraction of powders, which were dispersed in copper grids of 300 mesh; the accelerated electron beam was at 100 kV and 80 μA to produce bright field images. Transport properties of the samples were analysed by impedance spectroscopy, over the frequency range 5 Hz–13 MHz, using a Hewlett-Packard HP4152A impedance analyser, with an applied voltage of 0.1 V. Conductivities were measured over a temperature range 250–1000 °C. At each temperature, at least 1 h was allowed before measurements to ensure thermal equilibration of the sample.

A structural model for the unit cell of the new phase was built. It was used the CASTEP software [16], which is based on a wave plane method and a gradient correlation approach and a Perdew Wang Enderbok functional at a wave plane basis of $5 \times 5 \times 5$ k-point set with an 340.0 eV energy cut off and a self-consistent tolerance of 1×10^{-6} eV/atom. Based on a single point energy calculation the density of states and the electrostatic potential isosurface were observed. The use of the program, as part of the Cerius^2 suite of Accelrys, allowed an easy way to interpret and illustrate the properties of the model.

3. Results and discussion

3.1. Phase identification and structural analysis

Alumina addition (10 wt%) in YSZ integrates Al^{3+} atoms in the lattice to form a distorted cubic structure leading to a tetragonal phase, which is obtained at 1100 °C. However, higher added concentrations of alumina (>10 wt%) produced the formation of the monoclinic phase. For the structural analysis, the fractional atomic coordinates initially proposed as isostructural model in the refinement were based on the ZrO_2 cubic phase [16]. However, double lines in many of the Bragg positions, led to a tetragonal lattice. Rietveld refinement results, for this compound, are shown in Fig. 1.

Excluding the background selected data points (70), only nine parameters were needed to obtain a good refinement of the compound, i.e. atomic coordinates (1), profile (1), cell (2), zero (1), scale factor (1) and thermal isotropic parameters (3). Table 1 summarises the refined parameters, where low-fitting parameter values may be observed . Additional attempts were carried out to improve the refinement, including the possibility of a non-stoichiometric compound, however the effect of oxygen vacancies on the peak intensities is too small, in conventional X-ray diffractometers, to be included in calculations.

Since the lattice parameters of this product do not correspond to any tetragonal ZrO_2 phase previously reported, it may be regarded as a new phase product. After refinement, atomic positions of this new phase product are shown in Table 2, whilst Miller indices of observed peaks may be found in Table 3. The extinction symbol allows identify that the tetragonal space group for this new phase compound is P42/ncm.

3.2. Description of the new structure

Most atoms in the structure occupy special positions, only the oxygen coordinate z, Wyckoff position (4e), needs

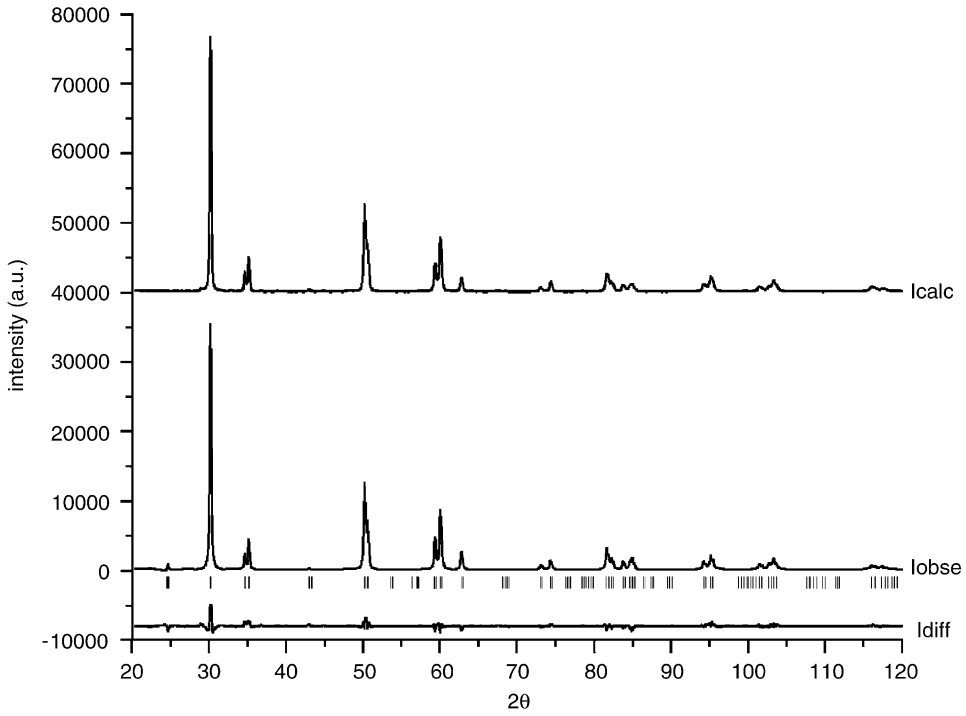

Fig. 1. (a) Calculated, (b) experimental and (c) difference X-ray diffraction patterns of novel YSZ–A tetragonal phase.

Table 1
Rietveld refinement parameters for novel YSZ–A tetragonal phase

Tetragonal cell (Å)	$a = 5.09964$ $c = 5.17488$
Space group	P42/ncm (138)
Formula per cell	$Z = 4$
Volume (Å^3)	134.580
Calculated density (g/cm^3)	6.08
Refined pattern (2θ range)	20–120
Step scan increment (2θ)	0.02°
Wavelength (Å)	1.54053 1.54431
No. of points	5001

$$R_{\text{Bragg}} = 100\sum_{i=1}^{i=n}\left|I_i^{\text{obs}} - I_i^{\text{calc}}\right| \Big/ \sum_{i=1}^{i=n} I_i^{\text{obs}} = 2.77,$$

$$R_{\text{F}} = 100\sum_{i=1}^{i=n}\left|I_i^{\text{obs}^{1/2}} - I_i^{\text{calc}^{1/2}}\right| \Big/ \sum_{i=1}^{i=n} I_i^{\text{obs}^{1/2}} = 3.19,$$

$$\chi^2(\text{Goodness of fit}) = (R_{\text{wp}}/R_{\text{e}})^2 = 2.8,$$

where

$$R_{\text{wp}} = 100\left(\sum_{i=1}^{i=n} w_i(y_i^{\text{obs}} - y_i^{\text{calc}})^2 \Big/ \sum_{i=1}^{i=n} w_i y_i^{\text{obs}^2}\right)^{1/2}, \quad R_{\text{e}} = 100\left[(N - P + C)/\sum_{i=1}^{i=n} w_i y_i^{\text{obs}^2}\right]^{1/2}.$$

to be refined, the value retained was 0.21 instead of 0.25. As a result, coordination polyhedra were deformed, referred to that of the cubic phase, Fig. 2.

Indeed, in the proposed structure, there are two different tetrahedrons, one centred in O_1 that is distorted and another centred in O_2 that is identical to that found in the cubic phase. Regarding the Zr polyhedra (8 oxygen first neighbours at 2.22 Å in cubic phase), a slightly distorted environment was found, where only a half of the distances correspond to the known cubic phase, this kind of distortion is also found in other tetragonal ZrO_2 phases [17].

3.3. Particle size

From TEM images, Fig. 3, the 3 mol% YSZ–Al_2O_3 particle size was determined to be in the range 50–100 nm, at 100 and 300 kX. However, agglomerated particles were observed in samples which were sintered at 1100 °C. The nanometric particle size was controlled, during the sintering process, by a slow increase in temperature. The electron diffraction patterns, which were obtained by TEM, corresponded to concentric bright points which are characteristics of nanometric polycrystalline material, the gaps between rings correspond to interplanar distances, which were indexed and then compared to those values which were obtained by the XRD-Rietveld refinement, results showed a good agreement for both data.

Table 2
Wyckoff positions, occupancies, fractional atomic positions and isotropic thermal parameters for YSZ–A tetragonal phase

Atom	Wyckoff position	N	x	y	z	B
Zr	4d	1.00	0.000	0.000	0.000	1.446
O1	4e	1.00	0.250	0.250	0.210	2.638
O2	4b	1.00	0.750	0.250	0.75	2.238

Table 3
X-ray powder diffraction data for novel YSZ–A tetragonal phase

n	2θ degrees	d-spacing (Å)	hkl	I_{calc}	I_{obs}
1	30.182	2.95854	1 1 1	100	100
2	34.638	2.58746	0 0 2	8	8
3	35.166	2.54981	2 0 0	14	14
4	50.190	1.81615	2 0 2	42	41
5	50.582	1.80299	2 2 0	21	20
6	59.340	1.55608	1 1 3	16	15
7	60.039	1.53962	3 1 1	31	30
8	62.759	1.47928	2 2 2	8	8
9	73.081	1.29371	0 0 4	3	3
10	74.339	1.27490	4 0 0	6	6
11	81.667	1.17802	3 1 3	13	12
12	82.277	1.17083	3 3 1	6	6
13	83.770	1.15372	2 0 4	4	4
14	84.681	1.14362	4 0 2	4	4
15	84.984	1.14031	4 2 0	4	3
16	94.244	1.05112	2 2 4	6	5
17	95.152	1.04348	4 2 2	12	12
18	101.480	0.99481	1 1 5	4	4
19	102.715	0.98618	3 3 3	4	3
20	103.335	0.98195	5 1 1	7	8
21	116.041	0.90808	4 0 4	4	4
22	117.393	0.90150	4 4 0	2	2

3.4. Transport properties

3.4.1. Electronic characteristics

Based on the quantum mechanics calculation, the electronic characteristics for the new tetragonal phase were

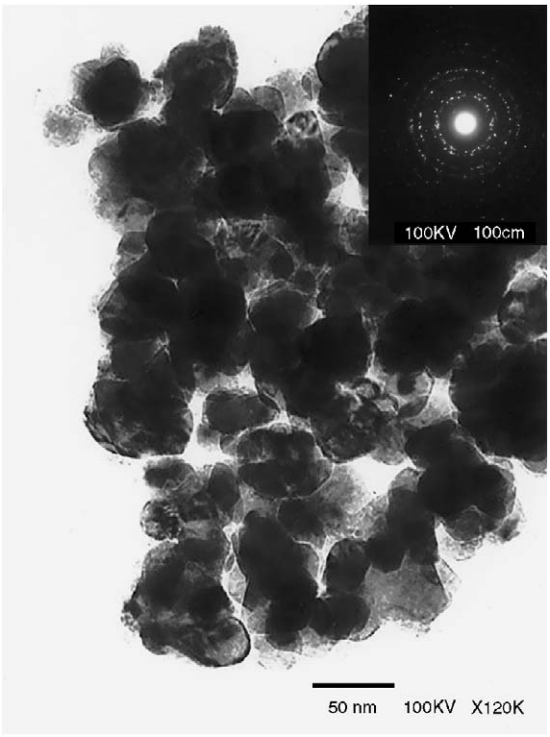

Fig. 3. (a) TEM image at 100,000 × and (b) diffraction electron pattern of YSZ–Al_2O_3 polycrystals with planar positions.

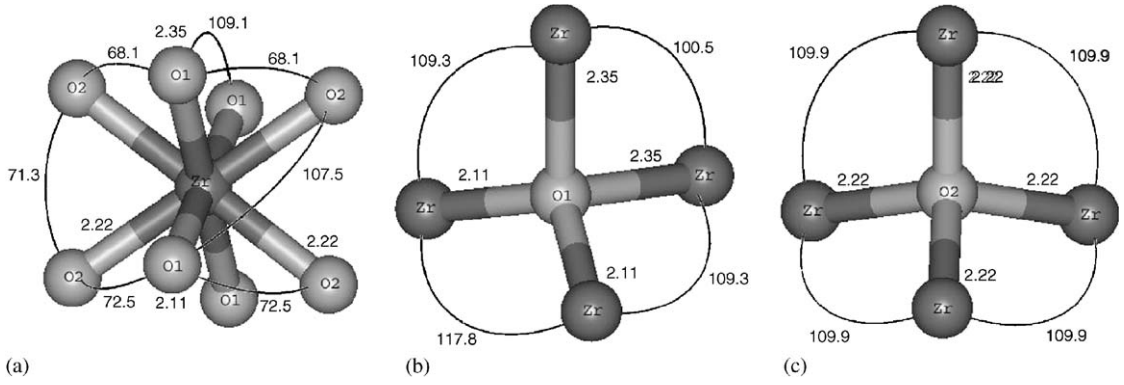

Fig. 2. Deformation of coordination polyhedron, found in novel YSZ–A tetragonal phase, which corresponds to the oxygen environment in a known cubic ZrO_2 phase.

analysed. As it can be observed, Fig. 4a, the charge density is mainly dominated by the oxygen atoms, producing well-defined channels and no continuous surfaces. Besides the electrostatic potential iso-surfaces, Fig. 4b, give us idea about the high homogeny of the potential in the unit cell, producing no polarisation in the density of states plot, Fig. 4c. In this phase, there are no free electrons as for the other ZrO_2 phases inducing a good basis for the ionic conduction but not for electron conductivity.

3.4.2. Ionic conduction

The addition of Y_2O_3 and Al_2O_3 to ZrO_2 produces vacancies along the structure. The substitution mechanism may be written as (3.4.2.1) and (3.4.2.2)

$$Y_2O_3 \rightarrow 2Y'_{Zr} + V'_O + 3O^{\times}_O,$$

$$Al_2O_3 \rightarrow 2Al'_{Zr} + V'_O + 3O^{\times}_O.$$

The partial substitution of Zr by Al^{3+} and Y^{3+} and the small particle size not only modified some features in the tetragonal structure of zirconia but also, the transport responses. This can be associated to the production of oxygen vacancies through the lattice, consequently, the replacement of zirconia cations by (3+) charge, produces a transport mechanism by vacancies of oxygen ions in the novel tetragonal zirconia phase. Impedance plots are shown in Fig. 5.

4. Conclusions

By using the co-precipitation method a new zirconia/alumina, YSZ/Al_2O_3 (90/10 wt%), tetragonal phase was obtained. Rietveld refinements indicated that this new tetragonal phase is based on antisymmetric tetrahedra that produce an elongated unit cell in comparison with previous reported phases. TEM images showed a homogenous compound with nanometric clusters ranged from 50 to 100 nm, which are made of smaller particles (3–10 nm). Results from impedance spectroscopy and density of states

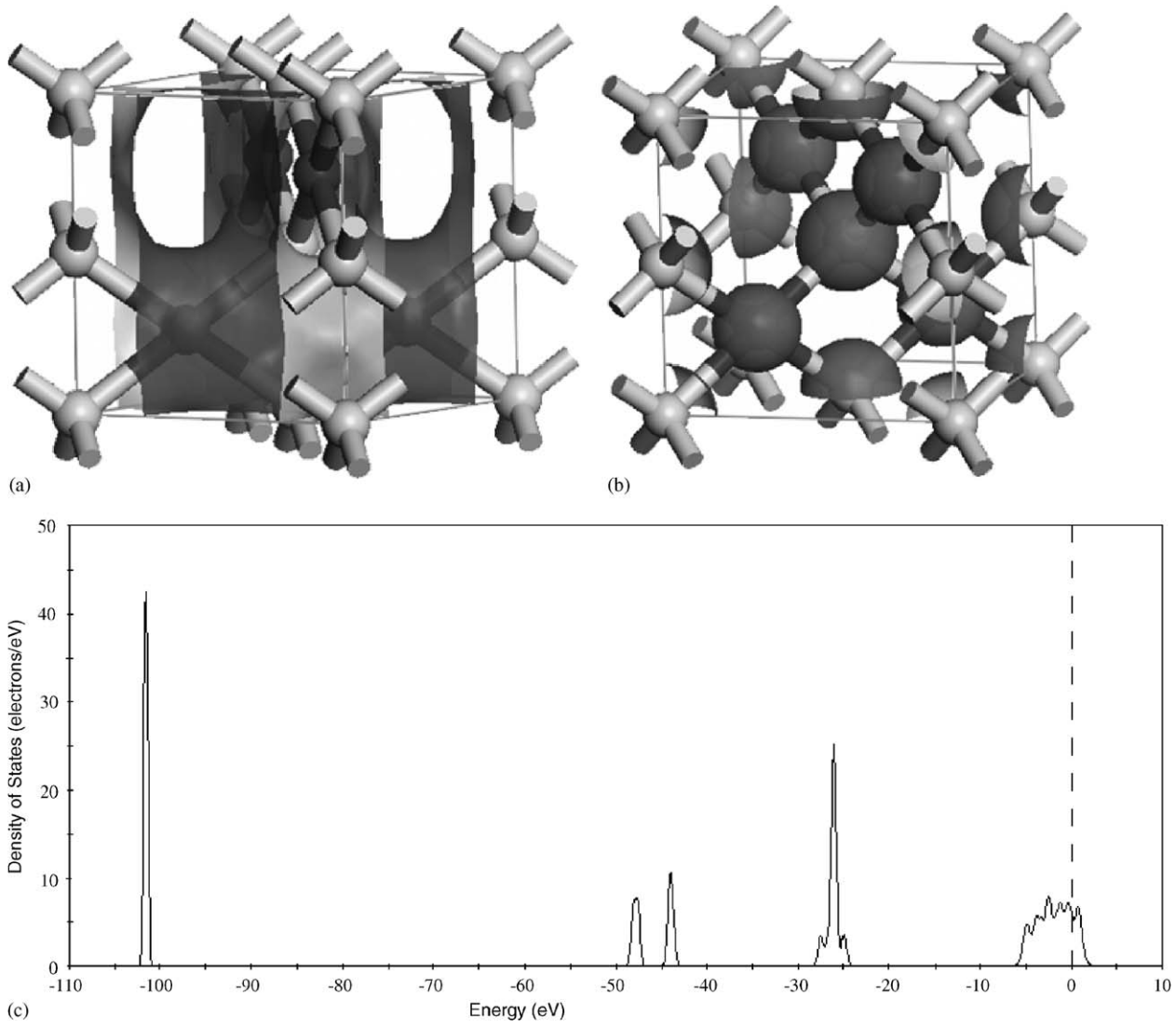

Fig. 4. Quantum mechanics unit cell calculation for the new tetragonal phase. (a) Charge density, (b) electrostatic potential of iso-surfaces and (c) density of states for the crystal structure.

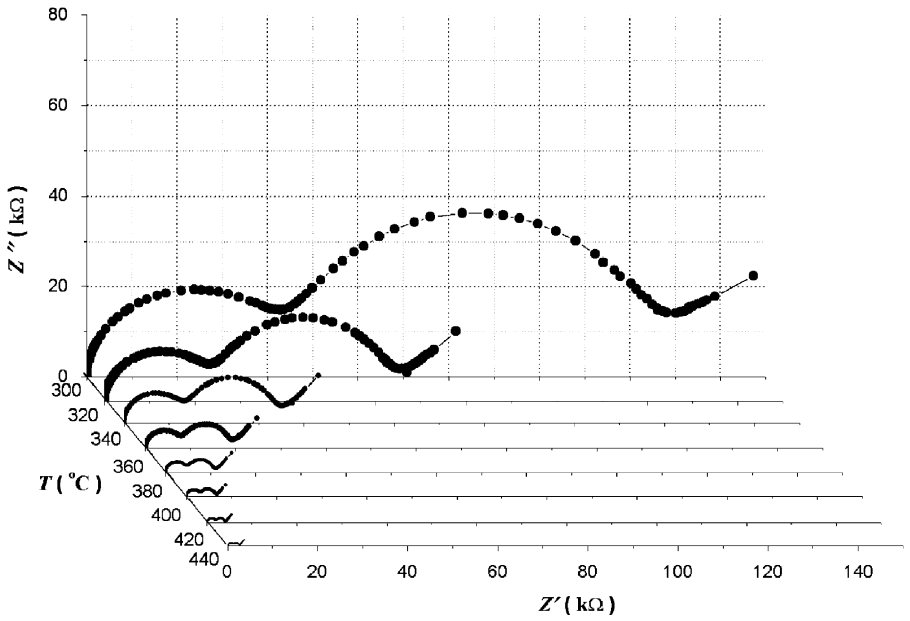

Fig. 5. Impedance plots of novel YSZ–A tetragonal phase, as a function of temperature.

for the crystal structure indicated that this new zirconia/alumina phase exhibits interesting transport properties not electronic but ionic conductivity, which is associated to oxygen vacancies in a stable tetragonal structure.

Acknowledgments

Authors thank Leticia Baños-López and Carlos Flores-Morales, IIM-UNAM, for their technical assistance.

References

[1] F. Boulc'h, L. Dessemond, E. Djurado, Solid State Ionics 154 (2002) 143.
[2] A.J. Feighry, J.T.S. Irvine, Solid State Ionics 121 (1999) 209.
[3] M. Dokiya, Solid State Ionics 152–153 (2002) 383.
[4] J. Drennan, G. Auchterlonie, Solid State Ionics 134 (2000) 75.
[5] Y. Wu, A. Bandyopadhyay, S. Bose, Mater. Sci. Eng. A 380 (2004) 349.
[6] L.J.M.J. Blomen, M.N. Mugerwa, Fuel Cells Systems, Plenum Press, New York, 1993, pp. 473–474.
[7] J. Kondoh, S. Kikuchi, Y. Tomii, Y. Ito, Physica B 262 (1999) 177.
[8] S.P.S. Badwal, F.T. Ciacchi, K.M. Giampietro, Solid State Ionics 176 (2005) 169.
[9] S. Kikkawa, A. Kijima, K. Hirota, O. Yamaguchi, Solid State Ionics 151 (2002) 359.
[10] J.C. M'Peko, D.L. Spavieri Jr., C.L. da Silva, C.A. Fortulan, D.P.F. de Souza, M.F. Souza, Solid State Ionics 156 (2003) 59.
[11] F. Ishizaka, T. Yoshida, S. Sakurada, O. Yamamoto, M. Dokiya, H. Tagawa, (Eds.), Proceedings of the International Symposium on SOFCs, Nagoya, Japan, November 13–14, 1989 Science House, Tokyo, 1989, pp. 172–176.
[12] F.J. Esper, K.H. Friese, H. Geier, N. Claussen, M. Ruhle, A.H. Heuer (Eds.), Science and Technology of Zirconia, American Ceramic Society, Columbus, OH, 1984, p. 528.
[13] F. Ishizaki, T. Yoshida, S. Sakurada. Proceedings of the Electrochemical Society. Fall Meeting, 1989, p. 3.
[14] D.Z. de Florio, R. Muchillo, Solid State Ionics 123 (1999) 301.
[15] J. Rodriguez-Carvajal, "computer program FullProf, version 3.51." Laboratoire Leon Brillouin. CEA. CNRS, Grenoble, France 1998.
[16] X. Zhao, D. Vanderbilt, Phys. Rev. B. 65 (075105) (2002) 1.
[17] F.J. Torres, J.M. Amigó, J. Alarcón, J. Solid State Chem. 163 (2002) 34.